Electronic Supplementary Material (ESI) for Nanoscale Advances.
This journal is © The Royal Society of Chemistry 2023

Electronic Supporting Information:

Modeling size and edge functionalization of MXene-based quantum dots and their effect on electronic and magnetic properties

Barbora Vénosová and František Karlický*

Department of Physics, Faculty of Science, University of Ostrava, 30. dubna 22, 7013 Ostrava, Czech Republic. E-mail: frantisek.karlicky@osu.cz

The hexagonal Ti_2CO_2 QDs considered in this work are shown in Figure S1 where $Ti_{24}C_7O_{24}$ represents a bare structure without any edge functionalization. This nanodot is then partially ($Ti_{24}C_7O_{30}$) and/or fully saturated ($Ti_{24}C_7O_{36}$, hereinafter referred to as QD1) by oxygen atoms. The oversaturated QDs (as $Ti_{24}C_7O_{42}$ or $Ti_{24}C_7O_{48}$) were spontaneously dissociated. Besides the dynamical stability of the geometrical structures (positive eigenvalues of the Hessian), the thermodynamic stability of QDs was considered by two means: according to the binding energy and the principle of maximum hardness.[1] First of all, our spin unrestricted calculations show that for all Ti_2CO_2 QDs models ($Ti_{24}C_7O_{24}$, $Ti_{24}C_7O_{30}$ and/or $Ti_{24}C_7O_{36}$, QD1), the spin-polarized state represents the ground state with respect to the positive values of the relative energies (ΔE = total energy of the singlet - total energy of the quintet states). In addition, the binding energy E_b of the saturation of the O atoms at the edge of the MXQDs was calculated to compare the stability of different shapes (different numbers of edge atoms). This is calculated from:

$$E_b = ((E_{MXDQ}) - (E_B + nE_O))/N, \quad (1)$$

where E_{MXDQ}, E_B and E_O denote the total energies of the ground states of Ti_2CO_2-O, bare Ti_2CO_2 QD without edge functionalization and an isolated oxygen atom, respectively. n is the number of oxygen edge atoms and N is the total number of atoms in MXQDs. The Gibbs energy is calculated by the same formula. As shown in Table S1, the binding energies have values of -0.79 and -1.26 eV for $Ti_{24}C_7O_{30}$, and $Ti_{24}C_7O_{36}$(QD1). Thus, it is clear that the fully saturated ($Ti_{24}C_7O_{36}$, QD1) is more stable with a stronger Ti - O bond at the edge. This stability is also confirmed by the maximum hardness principle, based on which a molecule with a higher HOMO-LUMO energy gap is associated with greater stability. From Table

S1, it is evident that saturated systems increase Δ_g compared to the corresponding bare structures, with the highest value corresponding to fully saturated $Ti_{24}C_7O_{36}$ (QD1). It is also worth noting the slight deformation of the bare structure ($Ti_{24}C_7O_{24}$) where the Ti-O bond is elongated on the QD side-face and subsequently shifted to the edge. This is apparently an attempt to compensate for the lack of electrons on the edge after 0D reduction and to favor the functionalization of the QD edge (Figure S1 and Table S8).

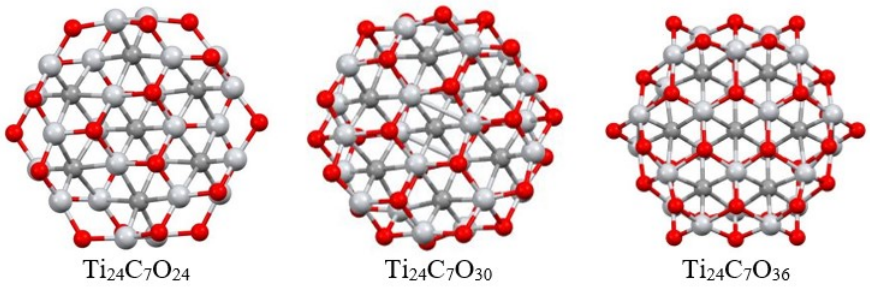

Figure S1: Optimized structure of bare Ti_2CO_2 QD without edge functionalization ($Ti_{24}C_7O_{24}$), with partially saturated edge ($Ti_{24}C_7O_{30}$) and with a fully saturated edge ($Ti_{24}C_7O_{36}$, QD1). Titanium, carbon and oxygen atoms are shown in light grey, dark grey and red, respectively.

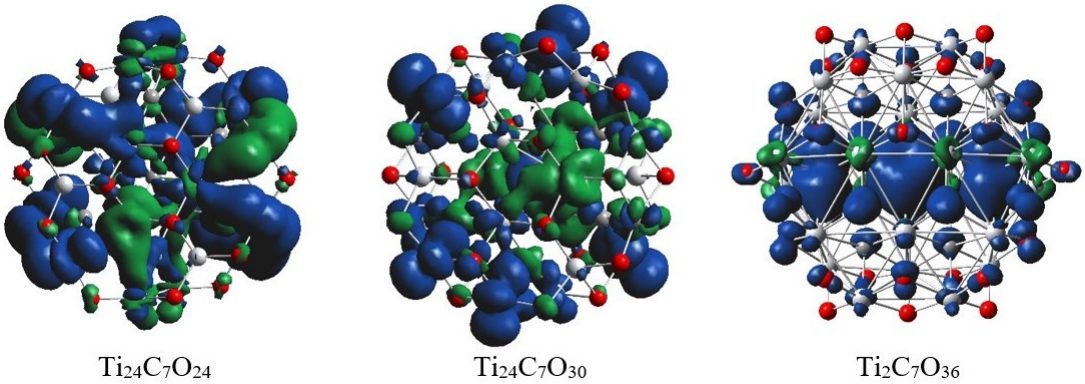

Figure S2: Spin density of the quintet states (m=4μ_B) of bare Ti_2CO_2 QD without edge functionalization ($Ti_{24}C_7O_{24}$), with partially saturated edge ($Ti_{24}C_7O_{30}$) and with a fully saturated edge ($Ti_{24}C_7O_{36}$, QD1). The isosurface values are 0.002 ebohr^{-3} (blue color represents positive and green color represents negative spin density). Titanium, carbon, and oxygen atoms are shown in light grey, dark grey, and red respectively.

Table S1: ωB97XD/6-31G** relative energy ΔE [eV] of singlet and quintet states (ΔE = total energy of the singlet - total energy of the quintet states), binding energies E_b [eV], ΔG Gibbs free energy change [eV], energy gap Δ_g [eV] of the quintet state and Ti-O length of bonds (in Å) of the ground states of Ti_2CO_2 QDs of the various number of edge atoms. The superscripts α and β stand for alpha and beta LUMO-HOMO gaps, respectively.

	ΔE	E_b	G	Δ_g	d_{Ti-O_e}
$Ti_{24}C_7O_{24}$	1.21	-	-	$4.21^{\alpha}/4.31^{\beta}$	-
$Ti_{24}C_7O_{30}$	0.78	-0.79	- 0.74	$4.98^{\alpha}/4.71^{\beta}$	1.92 - 2.15
$Ti_{24}C_7O_{36}$(QD1)	0.65	-1.26	-1.17	$7.29^{\alpha}/5.15^{\beta}$	1.77 - 2.05

Table S2: Comparison of calculated relative energies ΔE [eV] with respect to the electronic ground state (in bold) and $\langle S^2 \rangle$ expectation value for QD1. Both localized (6-31G**, Gaussian software) and plane-wave (PW) basis set (VASP software)[a] was used for comparison. Hybrid (ωb97XD, HSE06) and non-hybrid (PBE) levels of density functional theory were used. Calculation were performed in various spin state S represented by multiplicity M and magnetic moment m (in μ_B/QD).

S	M	m	ωb97XD/6-31G**		PBE/6-31G**		PBE/PW	HSE06/PW
			ΔE	$\langle S^2 \rangle$	ΔE	$\langle S^2 \rangle$	ΔE	ΔE
0	Singlet CS	0	0.65	0.00	**0.00**	0.00	**0.00**	0.03
0	Singlet OPS	0	0.03	1.97	-[b]	-	-	-
1	Triplet	2	0.21	2.95	0.23	2.02	0.11	
2	Quintet	4	**0.00**	6.05	0.30	6.02	0.21	**0.00**
3	Septet	6	2.10	12.05	2.55	12.02	2.29	-
4	Nonet	8	4.77	20.07	-	-	4.42	-

[a] The spin-polarized DFT level of theory in periodic boundary conditions together with the projector augmented-wave (PAW)[2,3] method as implemented in the Vienna *ab initio* Simulation Package (VASP)[3] (version 6.1) was used. Numerical details: PBE and HSE06 density functionals, 28 Å $\times$ 26 Å $\times$ 15 Å rectangular unit cell, Γ-point only version, the cut-off energy of 400 eV for the plane-wave basis set, the break condition for the electronic step is an energy difference of 1×10^{-5} eV, criterion on forces for optimization is 0.01 eV/Å.

[b] initial open shell state converted to the closed shell state

Table S3: Calculated ωB97XD relative energy ΔE [eV] of singlet and quintet states (ΔE = total energy of the singlet - total energy of the quintet states), $\langle S^2 \rangle$ expectation values for the quintet state, and energy gaps Δ_g [eV] for the singlet and quintet states of QD1 employing different basis sets. The superscripts α and β stand for alpha and beta LUMO-HOMO gaps, respectively.

	cc-pVTZ	6-311G**	6-31G**	def2-TZVP
ΔE	0.65	0.62	0.65	0.37
$\langle S^2 \rangle$	6.05	6.05	6.05	6.06
$\Delta_g^{Singlet}$	4.63	4.63	4.89	4.83
$\Delta_g^{Quintet}$	$7.22^{\alpha}/5.10^{\beta}$	$7.27^{\alpha}/5.13^{\beta}$	$7.29^{\alpha}/5.15^{\beta}$	$7.13^{\alpha}/4.98^{\beta}$

Table S4: For QD1, relative energy ΔE [eV] of singlet and quintet states (ΔE = total energy of the singlet - total energy of the quintet states), $\langle S^2 \rangle$ expectation values for the quintet state, and energy gaps Δ_g [eV] for the singlet and quintet states are compared using eight model density functionals. The superscripts α and β stand for alpha and beta LUMO-HOMO gaps, respectively. Calculations were performed *in vacuo* using the 6-31G** basis set.

	ΔE	$\langle S^2 \rangle$	$\Delta_g^{Singlet}$	$\Delta_g^{Quintet}$
ωB97XD	0.65	6.05	4.89	$7.29^{\alpha}/5.15^{\beta}$
CAM-B3LYP	0.66	6.04	3.29	$6.12^{\alpha}/4.10^{\beta}$
B3LYP	0.39	6.04	1.05	$3.26^{\alpha}/1.57^{\beta}$
HSE06	0.45	6.04	0.53	$3.24^{\alpha}/1.16^{\beta}$
PBE	-0.30	6.02	0.26	$2.08^{\alpha}/0.30^{\beta}$
BLYP	-0.28	6.02	0.24	$2.01^{\alpha}/0.31^{\beta}$
M06L	-0.21	6.02	0.36	$2.26^{\alpha}/0.39^{\beta}$
RevTPSS	-0.30	6.02	0.29	$2.17^{\alpha}/0.34^{\beta}$

Table S5: Magnetic moment on carbon atoms (see definitions in Figure S3) obtained from Mulliken population analysis (in μ_B) of the QD1 quintet state with magnetic moment 4 μ_B using different model density functionals.

	ωB97XD	cam-B3LYP	B3LYP	HSE06	PBE	RevTPSS	BLYP	M06L
C1	0.03	0.04	0.06	0.06	0.22	0.23	0.22	0.19
C2	0.03	0.04	0.06	0.06	0.22	0.23	0.22	0.19
C3	0.80	0.79	0.72	0.74	0.24	0.26	0.24	0.33
C4	1.40	1.36	1.21	1.23	0.88	0.85	0.95	1.33
C5	0.80	0.79	0.72	0.74	0.24	0.26	0.25	0.33
C6	0.03	0.04	0.06	0.06	0.22	0.23	0.22	0.19
C7	0.03	0.04	0.06	0.06	0.22	0.23	0.22	0.19

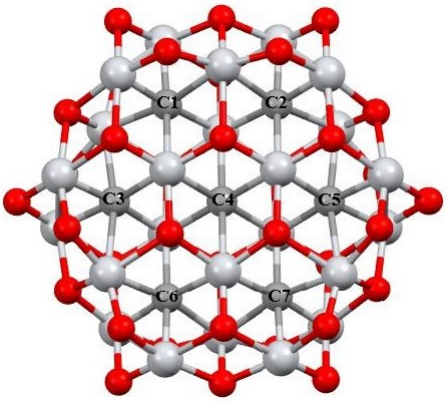

Figure S3: The optimized QD1 structure with labeled arrangement of carbon atoms. Titanium, carbon, and oxygen atoms are shown in light grey, dark grey, and red, respectively.

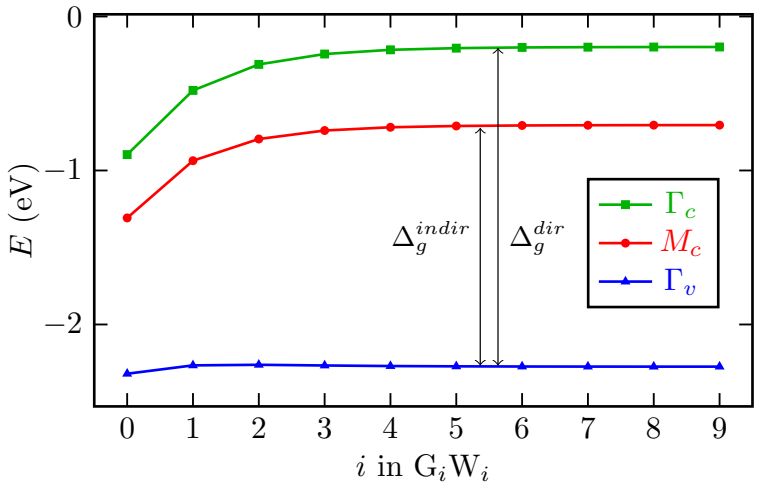

Figure S4: The quasiparticle gap Δ evolution with GW iterations of its eigenvalues (evGW variant of GW method) demonstrated on valence ("v") band maximum and conduction ("c") band minimum. Both direct ("dir", $\Gamma_v \rightarrow \Gamma_c$) and indirect ("indir", $\Gamma_v \rightarrow M_c$) gaps are opened significantly with iterations $i = 0 \rightarrow 9$: $\Delta_g^{dir} = 1.82$ eV $\rightarrow 2.47$ eV and $\Delta_g^{indir} = 1.32$ eV $\rightarrow 1.82$ eV ($cf.$ also Figure 3 of the main text). We note that our GW calculations with a "standard" setting[4] were renormalized to well-converged precise values of G_0W_0 of Ding et al.[5]

Table S6: Bond lengths (in Å) of Ti_2CO_2 QDs in ground states of different sizes. The subscripts i and s stand the bond lengths in the interior and in the side-face, respectively.

	QD1	QD2	QD3	QD4
Ti-C_i	2.25 - 2.37	2.07 - 2.30	2.09 - 2.22	2.12 - 2.21
Ti-C_s	1.97 - 2.43	1.90 - 2.43	1.88 - 2.43	1.97 - 2.43
Ti-O_i	1.76 - 1.94	1.76 - 1.94	1.79 - 1.98	1.88 - 1.98
Ti-O_s	1.80 - 2.11	1.80 - 2.11	1.80 - 2.11	1.80 - 2.11

Table S7: ωB97XD/6-31G** Multiplicity M, total magnetic moment μ and sum of spin down and spin up of partial magnetic moment on atoms obtained from Mulliken population analysis (in μ_B) of Ti_2CO_2 QDs of various sizes.

	QD1				QD2			
M	Triplet	Quintet	Septet	Nonet	Triplet	Quintet	Septet	Nonet
m	$2\mu_B$	$4\mu_B$	$6\ \mu_B$	$8\ \mu_B$	$2\mu_B$	$4\mu_B$	$6\ \mu_B$	$8\ \mu_B$
Ti	-0.20	-0.20	0.93	2.05	-0.18	-0.40	0.66	2.01
O	0.66	1.07	1.16	1.50	0.58	1.18	1.61	1.42
C	1.54	3.13	3.91	4.45	1.60	3.17	3.71	4.52
	QD3				QD4			
M	Triplet	Quintet	Septet	Nonet	Triplet	Quintet	Septet	Nonet
m	$2\mu_B$	$4\mu_B$	$6\ \mu_B$	$8\ \mu_B$	$2\mu_B$	$4\mu_B$	$6\ \mu_B$	$8\ \mu_B$
Ti	-0.25	-0.52	0.64	1.56	-0.26	-1.71	-*	- *
O	2.23	3.67	3.87	5.06	2.23	5.57	-*	-*
C	0.03	0.83	1.49	1.40	0.03	0.14	-*	-*

*spin states were not calculated

Table S8: Bond lengths (in Å) of QD1 in ground states with different edge functionalization. The subscripts i and s stand the bond lengths in the interior and in the side-face, respectively.

	Bare	O	F	OH
Ti-C_i	1.98 - 2.15	2.25 - 2.37	2.07 - 2.23	2.09 - 2.27
Ti-C_s	1.79 - 2.46	1.97 - 2.43	1.94 - 2.35	1.94 - 2.40
Ti-O_i	1.80 - 2.05	1.76 - 1.94	1.79 - 2.18	1.79 - 2.13
Ti-O_s	1.81 - 3.60	1.80 - 2.11	1.79 - 1.95	1.78 - 1.98

Table S9: ωB97XD/6-31G** Multiplicity M, total magnetic moment μ and sum of spin down and spin up of partial magnetic moment on atoms obtained from Mulliken population analysis (in μ_B) of studied QD1 with different edge functionalization.

M	Triplet			Quintet				Septet		
m	2 μ_B			4 μ_B				6 μ_B		
	O	F	OH	Bare	O	F	OH	O	F	OH
Ti	-0.21	2.12	2.11	4.34	-0.20	4.01	4.18	0.93	6.13	6.34
O	0.44	0.06	-0.04	-0.25	0.82	-0.06	-0.03	0.91	-0.02	-0.03
C	1.54	-0.03	-0.07	-0.09	3.13	0.02	-0.15	3.91	-0.01	-0.33
E	0.23	-0.08	0.01	-	0.25	-0.03	0.00	0.26	-0.07	0.02

Notes and references

[1] R. G. Pearson, *Accounts of Chemical Research*, 1993, **26**, 250–255.

[2] P. E. Blöchl, *Phys. Rev. B*, 1994, **50**, 17953–17979.

[3] G. Kresse and D. Joubert, *Phys. Rev. B*, 1999, **59**, 1758–1775.

[4] GW calculations by the VASP code using $N_{\mathrm{B}} = 384$ number of bands is (24 of them updated in GW), plane-wave energy cut-off $E_{\mathrm{cut}} = 500$ eV, GW cut-off $E_{\mathrm{cut}}^{\mathrm{GW}} = 200$ eV, $\Delta z = 20$ Å distance to perpendicular image, and $18\times18\times1$ k-point grid.

[5] Y.-m. Ding, X. Nie, H. Dong, N. Rujisamphan and Y. Li, *Nanoscale Advances*, 2020, **2**, 2471–2477.